CONSIDERATION OF AERODYNAMIC EFFECTS OF BLADE ROTATION AS COMPUTED WITH URANS IN LOAD SIMULATIONS WITH BEM

Stefan Hauptmann
Endowed Chair of Wind Energy
Universität Stuttgart, Germany
hauptmann@ifb.uni-stuttgart.de

Swen Streiner
Aero Dynamik Consult GmbH
Neuhausen, Germany
streiner@aero-dynamik.de

Felix Kunert
Endowed Chair of Wind Energy
Universität Stuttgart, Germany
felix.kunert@gmx.net

Martin Kühn
Institute of Physics
Universität Oldenburg, Germany
martin.kuehn@uni-oldenburg.de

Philipp Dörr
Institute of Aerodynamics and Gas Dynamics
Universität Stuttgart, Germany
doerr@iag.uni-stuttgart.de

Po Wen Cheng
Endowed Chair of Wind Energy
Universität Stuttgart, Germany
cheng@ifb.uni-stuttgart.de

Abstract

Load simulations for wind turbines are often based on the blade-element-momentum theory (BEM). This theory is based on a simplification of the underlying physics of rotor aerodynamics and makes use of 2-dimensional airfoil properties. Therefore, some relevant aerodynamic effects cannot be represented with this approach. These aerodynamic effects can be stationary or dynamic and assigned either to the global rotor flow or to the local flow within the boundary layer. The stationary effects that are related to the local flow within the boundary layer can be included into BEM simulations using so called 3 dimensional airfoil tables. Semi-empirical correction models have been developed to account for the particular effect. It is shown that relying on such correction models to account for 3 dimensional flow effects in the boundary layer is not precise enough to predict the loads on modern wind turbines under certain conditions. Therefore, a method is described to account for all relevant stationary effects in the boundary layer that are related to rotor rotation in BEM-based load simulations. The presented approach makes use of 3 dimensional URANS CFD simulations of a wind turbine rotor. The URANS simulations are used to extract 3 dimensional airfoil tables that can be used in load simulations based on the BEM approach. The 3D airfoil polars are explained in detail by means of the simulated flow field.

Keywords: Airfoil coefficients, Rotational augmentation, Stall delay, Load simulations

1. Introduction

For the design of large optimized modern wind turbines, detailed information about the aerodynamic and aeroelastic loads acting on them are required. Traditionally, the blade-element-momentum theory (BEM) is employed for load simulations as specified in the standards by GL [1] or IEC [2]. The BEM approach is based on simplified physics of rotor aerodynamics and relies on lift (C_l), drag (C_d) and moment (C_m) coefficients determined from 2D simulations or measurements. Due to these simplifications, this approach cannot represent the complex 3D flow and its interaction with the rotor rotation. On the one hand the corresponding phenomena can be divided into either stationary or dynamic flow effects. On the other hand these flow effects are either correlated with the boundary layer on the blade or the global rotor flow effects associated with the non-uniform and time-dependent induction factor and the consideration of the wake.

1.1 Rotational effects on local flow

This project focuses on the stationary local flow effects. The 2D airfoil data has to be modified to account for three-dimensional and rotational effects of the rotor blade boundary

layer. Through measurements it was found that maximum lift coefficients $c_{l,max,3d}$ are much higher (than the 2D coefficients $c_{l,max,2d}$) towards the rotational axis of a rotating blade and occur at higher angles of attack [3]. This effect of "stall-delay" and "post-stalled higher lift coefficients" can be ascribed to a combination of several physical effects [20]:

- A spanwise gradient of the dynamic pressure can be found on a rotating blade because of a dependency of the dynamic pressure on the rotational velocity and therefore the radius of the blade section. This gradient leads to a force on the boundary layer at the inner part of the blade acting in spanwise direction pointing outwards.

- The rotational effects can also be ascribed to inertial forces. The centrifugal force causes a spanwise pumping effect, known as "centrifugal pumping" leading to thinning of the boundary layer.

- The Coriolis force in the cross-flow leads to a beneficial pressure gradient along the profile and therefore tends to delay separation close to the axis of rotation.

1.2 Consideration of local flow phenomena

Several researchers like Snel [4] or Du and Selig [5], developed semi-empirical 3D correction models based on the computations of the 3D boundary layer flow. An improved approach for load simulations able to solve the complex flow phenomena described above is provided by 3-dimensional unsteady RANS (URANS) computations [6]. This method can also consider aeroelastic effects by including the fluid-structure interaction as demonstrated by Streiner [7]. Since such simulations consume a great deal of computational time it is, at least for the present, not yet realistic to simulate all the load cases as defined in the guidelines with such an approach.

This paper proposes a method to use 3D URANS simulations for the derivation of 3D airfoil tables used in load simulations with BEM. 2D airfoil coefficients depend on the angle of attack and also on the Reynolds number [8]. In case of 3D airfoil polars, there is also the rotational speed that has an influence on the coefficients. The stationary local flow phenomena, introduced as stall-delay and post-stall higher lift coefficients as well as the 3-dimensional tip flow are considered in such 3D coefficients.

2. Method

The presented research is based on a generic wind turbine with a rated power of 2.75MW and a rotor diameter of about 80m. This turbine is referred to as the reference turbine in this paper.

3-dimensional URANS simulations of the reference rotor are performed using the CFD code FLOWer [19]. Different turbulence models are available in FLOWer. However, due to good experiences in former studies [7] the k-ω SST turbulence model is the sole model used for the present study. In previous projects (e.g. Streiner [6]) similar URANS computations have already been performed and validated using the same grid of the considered reference turbine. The overall setup consists of the main grid components blade, hub and background grid, leading to a total number of about 10 million grid points. An insight to the grid setup is given in the following figure 1.

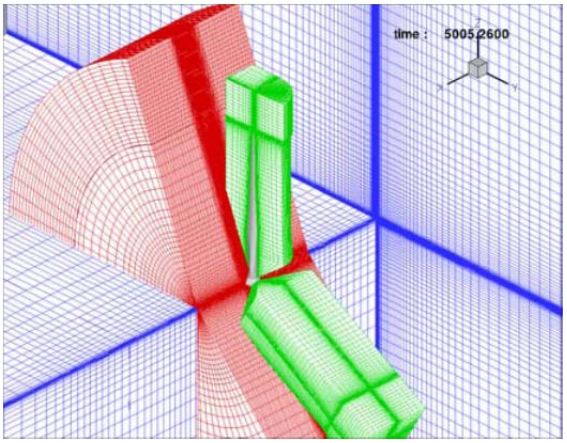

Fig.1: Grid setup showing blade (green), hub (red) and background grid (blue) [7]

The applied technique to extract 3D airfoil polars, the so called "reduced axial velocity method" was described by Streiner [9] and is based on Hansen [10]. For this approach a CFD simulation run has to be carried out to obtain the airfoil coefficients C_l, C_d and C_m for all the spanwise locations of the blade. The airfoil coefficients have to be calculated for different angles of attack, Reynolds numbers and rotational velocities. For each combination of those parameters, an individual CFD computation has to be carried out. Due to this, the number of required CFD simulation runs becomes large easily. Therefore, the effect of multiple Reynolds numbers was not examined

individually and the airfoil tables are calculated for two different rotational speeds at Ω = 1rad/s and Ω = 2rad/s only. The angle of attack is evaluated for the most interesting region from about α_{eff} = -20° to α_{eff} = 40°. 13 different angles of attack are evaluated for each rotational velocity, resulting in a total of 26 simulation runs. The extrapolation to capture a 360° airfoil polar was performed using the approach of Viterna [11]. These 3D airfoil polars are explained and validated with regard to the 3D flow phenomena. In addition, 2D XFOIL calculations are performed to generate 2D airfoil tables. These 2D airfoil polars are corrected by the Du and Selig model mentioned above and serve as the basis for validations.

3. Results

3.1 Evaluation of the local flow field

The URANS simulation results are used to discuss the relevant 3D flow effects due to the blade rotation. Therefore the flow field close to the blade surface is analyzed. The complex 3 - dimensional flow field around a rotor blade is illustrated in figure 2. The flow situation is shown for a wind speed of v_{wind} = 10m/s, a rotor speed of Ω = 2rad/s and a pitch angle of Θ = 0° which corresponds to an angle of attack of about $\alpha_{eff} \approx 5°$ for most spanwise positions.

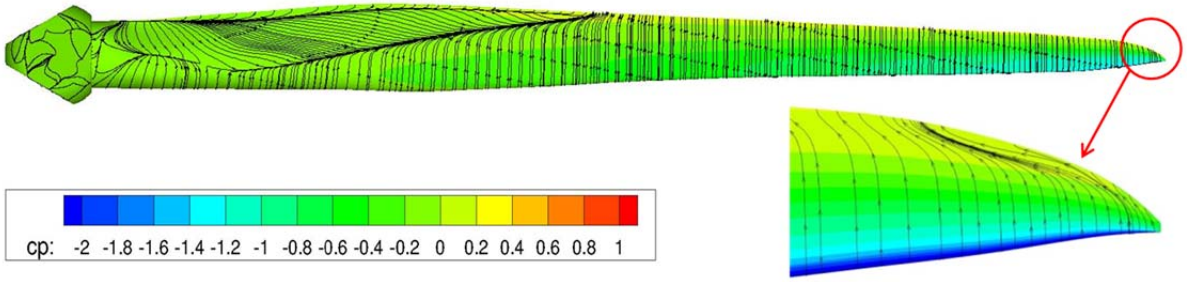

Fig 2: Streamlines at the rotor blade suction side (v_{wind} = 10m/s, Ω = 2rad/s, Θ = 0°)

Figure 2 shows the general effects of a 3D flow on a rotating blade. Close to the blade root, a region of boundary layer separation can be identified. The streamlines in the separated flow are pointing towards the blade tip which can be explained by a spanwise pressure gradient, as well as centrifugal pumping.

In the center part from about 50% to 90% span of the rotor blade the flow is attached and the streamlines are parallel. Therefore, it can be concluded that quasi-2D flow conditions can be assumed.

Very close to the tip, attached flow conditions can be identified. Nevertheless, the streamlines are also affected by rotor rotation, but pointing to the inner part of the blade. This can be explained by the tip vortex from pressure to suction side.

The C_l, C_d and also C_m coefficients are evaluated at three representative spanwise locations: close to the blade root, close to 2/3 of the rotor radius and at a position near the blade tip. A comparison to XFOIL 2D polar data with application of the Selig and Du correction model and a 2D reference airfoil is presented.

3.2 Effects on the lift coefficients

The figures 3, 4, and 5 show C_l-α-polars at three different spanwise locations. The polars are determined using different approaches. The 3D polars that are extracted from the rotating 3D URANS computations using the reduced axial velocity method are presented. Also 2D data from the STABCON project [13] is presented. This 2D data was fitted to measurements of global loads of the reference wind turbine. Furthermore the 2D XFoil data that is 3D-corrected using the Du and Selig model is given for comparison. The 3D polars are plotted for two different rotational velocities of Ω = 1rad/s and Ω = 2rad/s

The 3D CFD polars close to the blade root show a significantly higher C_l value compared to the 2D polars for high angles of attack (post stall) and are dependent on the rotational velocity. This makes perfect sense since the centrifugal pumping effect and Coriolis forces have a significant influence on the separated boundary layer as described before. It can also be concluded that the semi-empirical correction model by Selig and Du predicts a similar trend, but the results differ significantly from the 3D CFD polars.

In the center part of the rotor blade the 3D polars and the 2D data are very similar. This result can be expected when considering the quasi-2D flow conditions as shown in figure 2.

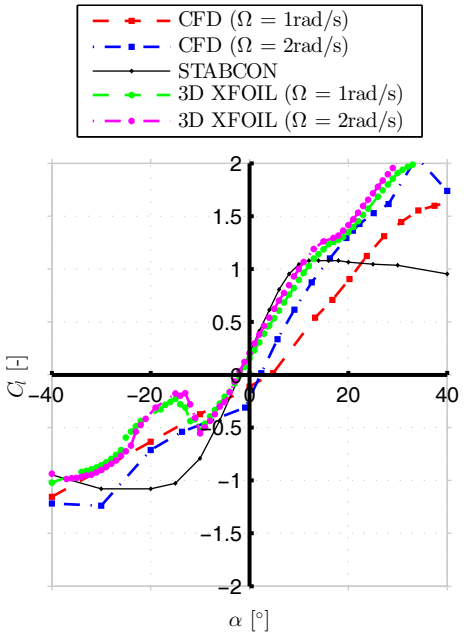

Fig 3: C_l-α polar at 1/4 span, representing 3 different methods for 2 different rot. velocities

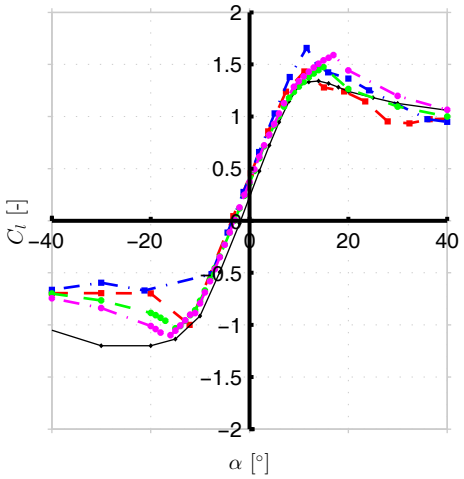

Fig 4: C_l-α polar at 3/4 span, representing 3 different methods for 2 different rot. velocities.

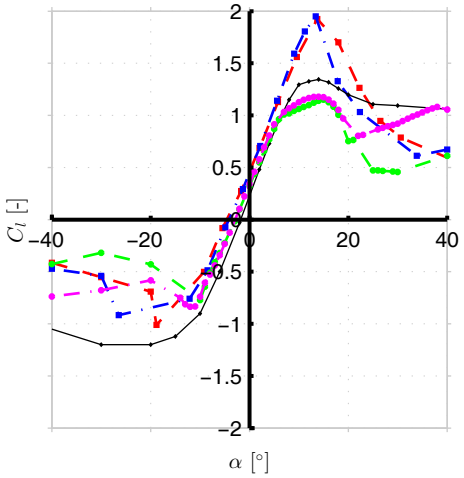

Fig 5: C_l-α polar at 4/4 span, representing 3 different methods for 2 different rot. velocities

Close to the tip, the 3D correction model differs from the 3D CFD results. The correction model predicts a decrease of C_l due to the tip vortex. In contrast the 3D CFD results show a significant increase of C_l. This effect is explained by means of the tapering at the blade tip [14] which is dominant in contrast to the existence of the tip vortex. This result demonstrates the need to solve the blade specific flow conditions instead of relying on general semi-empirical correction models.

3.3 Effects on drag coefficients

The effect of blade rotation on the drag coefficients is not yet evaluated conclusively [20]. The empirical correction model by Selig and Du predicts a decrease of drag for blade sections close to the root where an increase in $C_{l,max}$ and stall angle α_{Stall} is predicted. Since the large area of separation is expected to increase the pressure drag, an increase of the drag coefficient can be expected for sections close to the blade root.

Figures 6, 7, and 8 show the drag coefficients derived from the URANS simulations for the reference turbine at three spanwise positions, plotted as C_l- C_d polars.

Close to the blade root, the undetermined results that are found in the literature can be approved. Compared to the reference data derived from the STABCON project the XFOIL result, modified using the Selig and Du approach, shows a significant decrease of the drag coefficients as expected for this method. The results from the 3D URANS simulations are highly dependent on the rotational speed of the rotor blades. In general it can be concluded that the drag is significantly higher compared to the 2D reference. Nevertheless, for angles of attack close to the zero-lift angle the drag coefficient is increased compared to the 2D case for moderate rotational speeds (in this case Ω = 1rad/s) but decreased for a higher rotational speed (Ω = 2rad/s). To interpret this effect in more detail, additional simulations with rotational speeds in between the two considered have to be performed. In figure 6 it is also shown that the stall-characteristics differ significantly from the 2D case.

At about 2/3 of the blade span the stall characteristics and the drag coefficients look much more common and are comparable to the 2D case. This result was expected because of the interpretation of the streamlines shown in figure 2.

Close to the tip the drag coefficients in the 3D

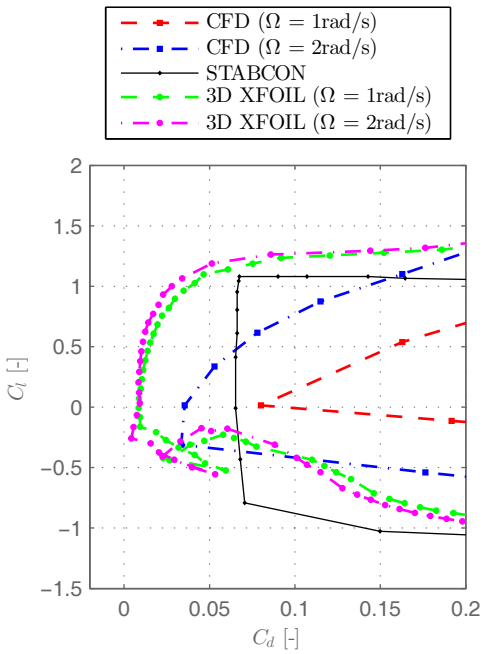

Fig 6: C_l- C_d polar at 1/4 span, representing 3 different methods for 2 different rot. velocities

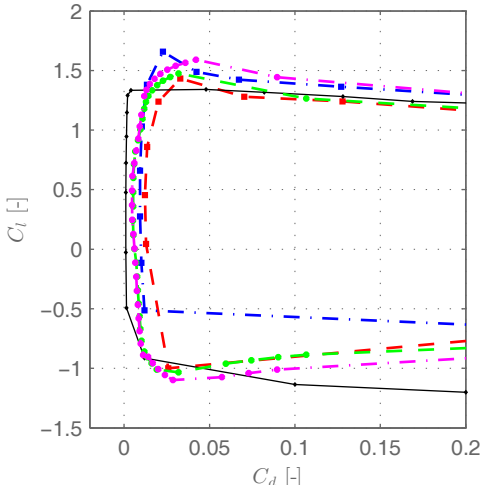

Fig 7: C_l- C_d polar at 3/4 span, representing 3 different methods for 2 different rot. velocities

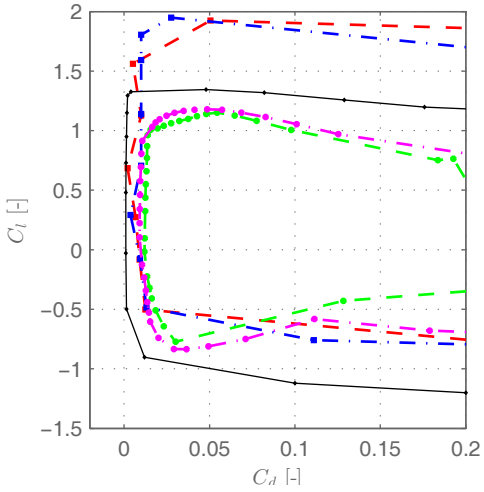

Fig 8: C_l- C_d polar at 4/4 span, representing 3 different methods for 2 different rot. velocities

case as predicted by the empirical correction model as well as by the 3D URANS simulations are higher compared to the 2D case. This effect has to be ascribed to the tip vortex that is shown in figure 2. The drag related to such tip vortices is well known as the induced drag.

3.4 Effects on moment coefficients

The influence of 3-dimensional effects due to blade rotation on the moment coefficients is not considered in any empirical correction model and has not been analyzed before to the author's knowledge. Nevertheless the moment coefficients are of high importance for wind turbine simulation especially in regard to the prediction of aeroelastic stability.

In figures 9-15 the moment coefficients C_m are presented for a reference point of the airfoil at 25% of chord length. Figures 9-12 show the spanwise distribution of the moment coefficients for different angles of attack and a rotational speed of Ω = 2rad/s. The STABCON reference airfoil and the XFOIL data are almost identical, because the correction model to account for 3D effects does not modify the moment coefficients at all. An outlier in the XFOIL data is caused by numerical problems with the specific airfoil.

It can be noticed that especially for lower angles of attack, the 3D URANS results do match the 2D moment coefficients accurately for the majority of spanwise positions. Only close to the root and - especially for higher angles of attack - close to the tip the 3D results differ in regard to the 2D case. The area of separated flow occurring already for small angles of attack due to rotation in the root section of the blade has a dominating effect on the moment coefficients. Nevertheless, the moment coefficient close to the root is not very important for the aeroelastic stability of the rotor blade.
In the very outer part (r > 99% R) of the rotor blade, the 3D moment coefficients differ significantly from the 2D case. This cannot be explained by separation, because the differences occur for small angles of attack with associated attached flow conditions. Instead the tip vortex has a dominant effect on the center of pressure of the airfoil. To describe the rotational effects on the moment coefficients on the basis of the angle of attack the C_m - α polars are plotted for different radial positions analogue to the C_l - α and C_l - C_d polars. The airfoil reference point for the moment coefficients is chosen as the 25% chord position that is close to the neutral

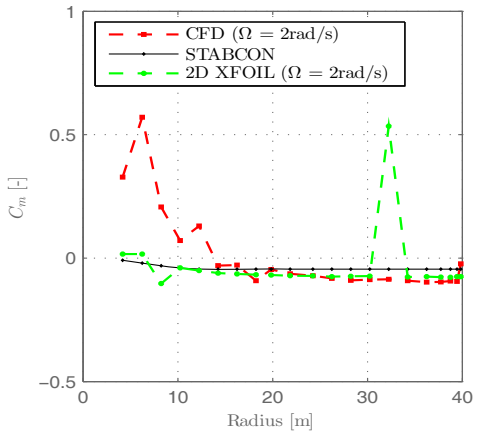

Fig 9: Spanwise distribution of C_m for α = -5°

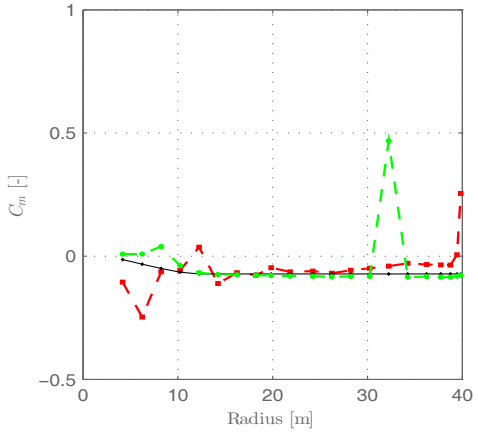

Fig 10: Spanwise distribution of C_m for α = 0°

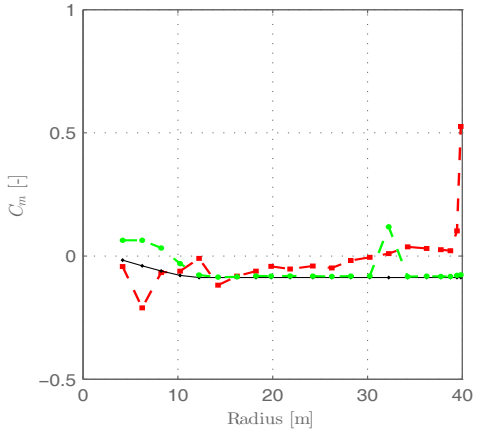

Fig 11: Spanwise distribution of C_m for α = 5°

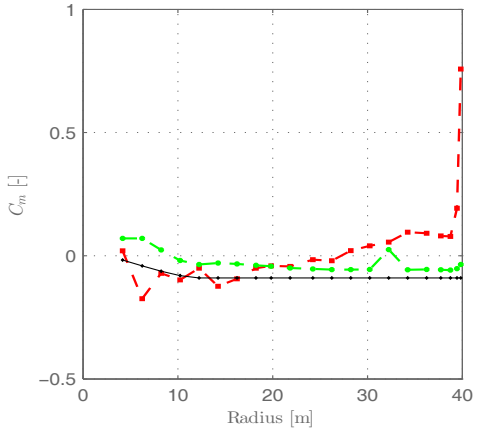

Fig 12: Spanwise distribution of C_m for α = 10°

point for most airfoils. Therefore, a constant distribution of the moment coefficients over the blade span has to be expected. Such a distribution is shown by all approaches for all angles of attack within the range of attached flow. Only in stalled conditions, the results differ significantly.

The very large moment coefficients that occur very close to the tip as shown in figures 10-12 are not found in the polar plotted in figure 15. The plotted polar originates from a spanwise position of 99% while the increase in moment coefficient is limited to the very outer part of the blade.

4. Conclusion and Outlook

This paper demonstrates how the local steady 3-dimensional flow phenomena computed using a 3D URANS approach can produce 3D airfoil tables to be used in load simulations with BEM. The lift coefficients simulated using the 3D URANS approach differ from the 2D data. This effect is well known and ascribed to a spanwise gradient of dynamic pressure due to the rotational speed as well as the effect of “centrifugal pumping” related to the Centrifugal and Coriolis forces. The empirical correction model from Selig and Du shows a similar trend, but is not able to cover the effects of rotational augmentation in detail for the reference turbine.

The influence of the 3D effect to the drag coefficient is not yet fully understood. The 3D drag coefficients predicted by the empirical correction model and the 3D URANS simulations differ. It can also be concluded that the rotational speed has an important and non-linear effect on the drag coefficient. For the moment coefficient no correction model exists at the moment. The 3D URANS simulations showed that this effect is not dominant and mainly related to angles of attack in stalled conditions.

Not all load cases defined in standards can be exactly determined using BEM, even with 3D airfoil tables, because of dynamic local flow phenomena such as dynamic stall, and also because of non-uniform induction factors. To overcome the limitations of BEM regarding the global flow phenomena, a non-linear lifting-line vortex wake method as developed e.g. by ECN [15] can be applied. To physically solve the dynamic stall effect, CFD calculations have to be performed. Even very detailed RANS solvers have difficulties to consider this phenomenon, because a

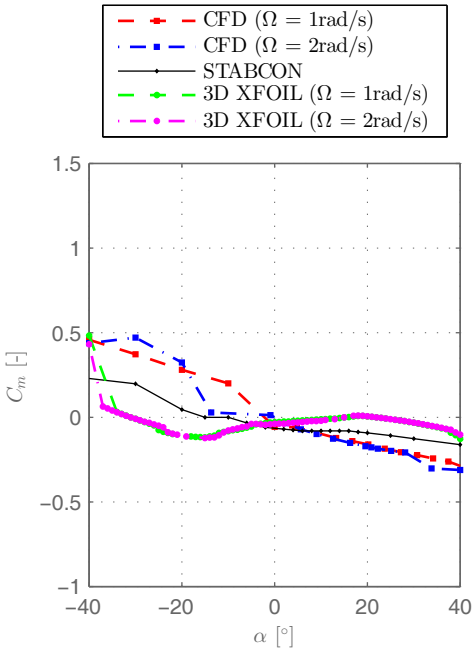

Fig. 13: C_m-α polar at 1/4 span, representing 3 different methods for 2 different rot. velocities

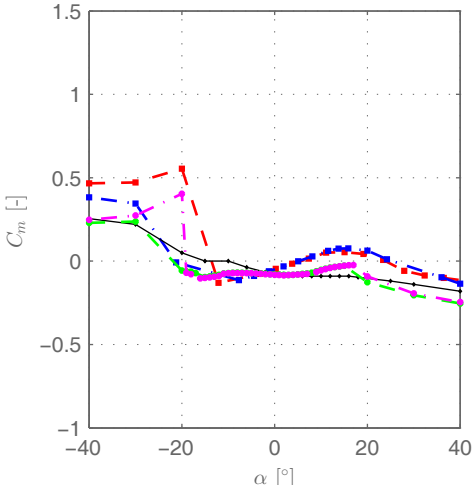

Fig 14: C_m-α polar at 3/4 span, representing 3 different methods for 2 different rot. velocities

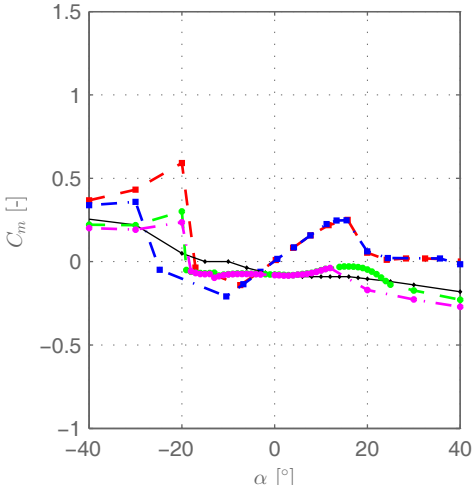

Fig 15: C_m-α polar at 4/4 span, representing 3 different methods for 2 different rot. velocities

prediction of the laminar-turbulent transition point is not trivial in such an approach [16].

References

[1] GL-Wind: “Guideline for the Certification of Wind Turbines“, Edition 2010

[2] IEC 61400-1: ”Wind turbine generator systems - Part 1: Design requirements“, third edition, August 2005

[3] Carcangiu C E et al: “CFD–RANS analysis of the rotational effects on the boundary layer of wind turbine blades“, Journal of Physics: Conference Series 75, 2007

[4] Snel H et al: “Sectional prediction of 3-D effects for stalled flow on rotating blades and comparison with measurements”, Proc. of EWEC 395–9, 1993

[5] Du Z, Selig M S: “The effect of rotation on the boundary layer of a wind turbine blade“, Renewable Energy 20 167–81

[6] Streiner S, Krämer E: “Aeroelastic Analysis of Wind Turbines Applying 3D CFD Computational Results” 2007 J. Phys.: Conf. Ser. 75

[7] Streiner S, Hauptmann S et al: "Coupled Fluid-Structure Simulations of a Wind Turbine Rotor", DEWEK08, Germany, 2008

[8] Lindenburg C: ”Investigation into Rotor Blade Aerodynamics” ECN-C-03-025, June 2003

[9] Streiner S: “Beitrag zur numerischen Simulation der Aerodynamik und Aeroelastik großer Windkraftanlagen mit horizontaler Achse“, Doctoral thesis, Stuttgart University, Stuttgart, 2010

[10] Hansen M O L: “Extraction of lift, drag and angle of attack from computed 3-D viscous flow around a rotating blade” Proc. of EWEC 499–502, 1997

[11] Viterna L A et al: “Theoretical and Experimental Power from Large Horizontal-Axis Wind Turbines”, NASA TM-82944. Washington DC, September, 1982

[12] Moriarty P J: “AeroDyn Theory Manual”, National Renewable Energy Laboratory, 2005

[13] Politis E S et al: “Benchmark calculations on the NM80 wind turbine”, Centre for Renewable Energy Sources, Pikermi, Greece, 2004 (Risø-I-2275(EN)). - Task 1 Technical Report

[14] Ferrer E, Munduate X: “Wind turbine blade tip comparison using CFD”, Journal of Physics, 2007

[15] Garrel A v: “Development of a Wind Turbine Aerodynamics Simulation Module”, Report ECN-C-03-079, ECN 2003

[16] Krumbein A: ”Transition Modeling in FLOWer - Transition Prescription and Prediction”, DLR Braunschweig

[17] Breton S-P: “Study of the stall delay phenomenon and of wind turbine blade dynamics using numerical approaches and NREL’s wind tunnel tests“, Doctoral thesis, Trondheim, June 2008

[18] Tangler J L: “The Evolution of Rotor and Blade Design”, AWEA WindPower 2000, Palm Springs, California

[19] FLOWer: "Installation and User Manual of FLOWer MAIN version FLOWer 1-2007.1.”, DLR Braunschweig, 2007 - Release 2007.1

[20] Lindenburg, C.: “Modelling of Rotational Augmentation Based on Engineering Considerations and Measurements, EWEC2004, London, Great Britain